ATTITUDE DETERMINATION, CONTROL AND OPERATING MODES FOR CONASAT CUBESATS

Valdemir Carrara[(1)], Hélio Koiti Kuga[(2)], Philipe M Bringhenti[(3)], and Manoel J M de Carvalho[(4)]

[(1)(2)(3)(4)] *Space Research National Institute-INPE, Av. dos Astronautas, 1758, São José dos Campos, SP, Brazil, 55-12-3208-6183, valdemir.carrara@inpe.br, helio.kuga@inpe.br, philipemassad@hotmail.com, manoel@crn.inpe.br*

Abstract: *CONASAT is being designed to gather environmental data like rain volume, temperature, humidity, air pollution, ocean streams, environmental hazards, etc. collected and transmitted to satellite by remote platforms on ground, and to retransmit them to the mission center. At least two identical satellites shall be launched, and, together with their antecessors SCD1 and SCD2 (Data Collecting Satellites 1 and 2, from Brazil) launched in 1993 and 1998, respectively, and still operating, they will provide large temporal resolution for environmental monitoring. In order to keep the costs low, CONASAT shall be based on CubeSat technologies. However, the large power required by onboard data transponder implied an arrangement of 8 CubeSat units in a single cubic one, with 230 mm size. All internal subsystems shall be duplicated in cold redundancy, in order to assure the reliability. In addition, in order to fulfill the power requirements, the attitude shall be Earth pointed, since the payload antenna will face to ground. Although there is no restraint in pointing requirements, a set of 3 off the shelf reaction wheels will be employed so as to assure satellite maneuverability and attitude stabilization. Attitude determination will rely in a set of 6 coarse sun sensors (one in each cube face) and a tri-axes magnetometer. QUEST or TRIAD algorithm together with Kalman filter will provide onboard attitude determination and estimation whereas attitude control will be based on a conventional PID, acting on the reaction wheels, and three magnetic coils necessary for wheel's de-saturation. Onboard software reliability is assured by minimizing the number of operating modes. Besides the nominal and stand-by modes (for Earth pointing and station keeping, respectively), the attitude acquisition mode and the safe mode for attitude de-tumbling shall be accomplish by means exclusively of the magnetometer (Bdot algorithm), course solar sensors and the torque coils. Since there is no complete attitude determination on the shadowed part of the orbit, the nominal mode is achieved only after Kalman filter convergence. This work will present the attitude control modes for CONASAT, as well as the transition conditions between modes. The results from the simulated attitude determination, estimation and control will be addressed, with focus on the attitude performance for both nominal and safe modes. This work shall constitute a base line that will guide the on-board control software development, integration, and qualification tests.*

Keywords: *Cubesat, satellite attitude determination, satellite attitude control, satellite operating modes.*

1. Introduction

The federal government of Brazil has invested since 1980 in the infrastructure necessary for the development, launching and operation of satellites, with in-house technology. This effort succeeded in 1993 and 1998 with the launching of the Data Collecting Satellites SCD1 and

SCD2, respectively. Although they were designed for a lifetime of just one year, both satellites are still operating and working properly at the time of this writing. Unfortunately, the development of launch vectors did not succeeded yet, although Brazil is still seeking for a solution by its own means.

The SCD main payload consists of a transponder that relays environmental data received from remote Data Collecting Platforms (PCD). The PCDs are spread throughout Brazilian territory, especially in difficult access sites, such as the Amazon forest and uninhabited areas in the center of the country. Both satellites have their attitude stabilized by rotation. Their attitude control system is very simple, based on magnetic coils activated by on-ground telecommands sent by the control station that drives the rotation axis to be aligned to the ecliptic normal, to ensure a good exposure of the solar panels to the Sun. The high SCDs longevity, allied to a large number of installed PCDs, created a dependency of the user's community with the environmental data. The continuity of the data collecting system was ensured with the launch of CBERS series (1, 2 and 2B), a remote sensing satellite of 1.5 ton, in join cooperation between Brazil and China. The CBERS satellites had, as secondary payloads, a transponder for the PCDs. However, the three CBERS already launched were decommissioned some years ago. With both SCD satellites also showing signs of failures, Brazil is seeking for ways to continue the data collection system using low cost satellites, such as the nanosats or CubeSats. Within this point of view, the National Institute for Space Research (INPE) has proposed to the Brazilian Space Agency (AEB), and had been approved, the development, construction, launching and operation of a constellation of CubeSats, named CONASAT, focused on environmental data collection.

Each CONASAT is configured as an 8U (CubeSat units) on a cubic arrangement, as seem in Figure 1. All the subsystems (power supply, attitude control, data handling and payload) are stored in a 2U configuration. All the subsystems are duplicated in other 2U unit in cold redundancy. The remainder 4 units are empty, but they provide the extra surface for the solar cells required by the power budget.

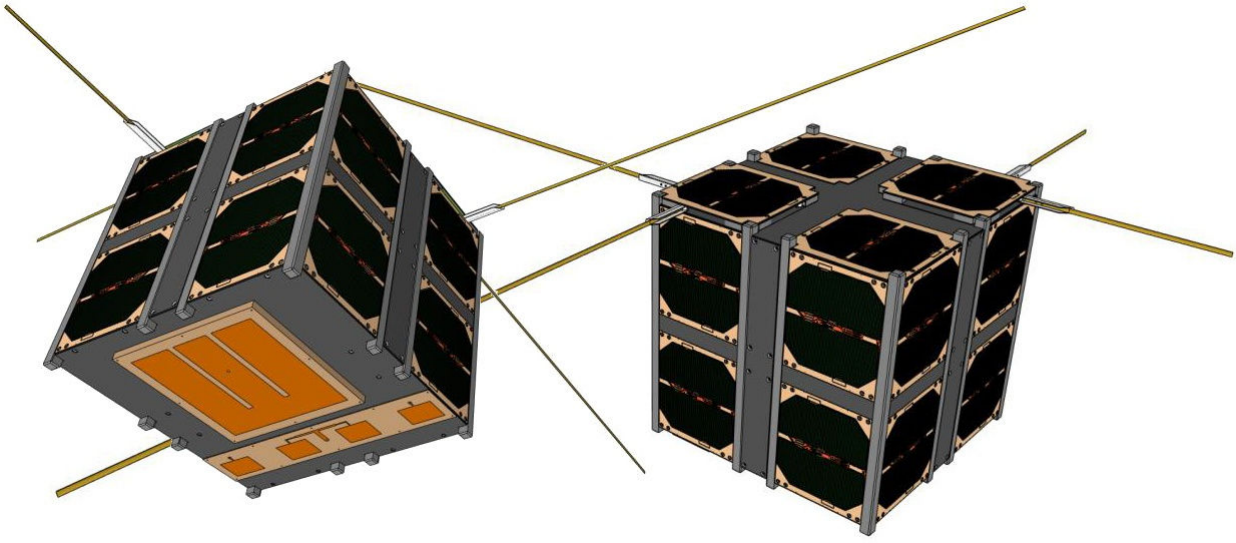

Figure 1. The CONASAT satellites are arranged in an 8U CubeSat configuration.

To ensure high performance and low power consumption the CONASAT will be provided with planar antennas required to receive data from the PCD platforms. These antennas are directional, and therefore should be pointed at the Earth, which requires that the attitude of the satellite is geo-pointed, to rotate around the pitch axis with a rotation every orbital period. The required pointing accuracy shall be around 5° from nadir. Although there is no requirement for pointing accuracy in the yaw axes, in this work it is assumed that the error around yaw shall also be less than 5°. Attitude determination will be performed using six analog sun sensors (in each satellite face), and a 3-axis magnetometer. A MEMS gyroscope will provide 3-axis angular velocity measurements. As for attitude control, the satellite will count with a set of three reaction wheels and 3 magnetic torque coils.

The satellite will operate in 3 distinct modes: nominal mode, in which the payload transponder is switched on; safe mode, in which the attitude is stabilized and controlled with magnetic torquers; and attitude acquisition mode, necessary to stabilize the satellite after orbit injection and to drive the attitude close to the nominal. Attitude acquisition shall also employ the magnetic actuators for attitude control. Besides these modes of operation, there is still the stand-by mode, in which the attitude is not controlled, but telemetry is sent and telecommands are decoded. Some additional assumptions were adopted in this work in order to enable attitude simulation. Firstly, because of the similarity of operations between the safe and attitude acquisition modes, they will be considered a single one; at least until the satellite detailed design allows to distinguish the differences between these modes. The pointing requirements for the safe and acquisition modes were established such that it will be possible to switch to the nominal mode when required without saturating the reaction wheels. For this an appointment with error less than 10° in the roll, pitch and yaw axes was adopted in the safe and acquisition modes.

This paper aims, therefore, to establish the attitude control laws for CONASAT and to perform a simulation to prove the efficacy of the controller. So as to achieve the control parameters, it was adopted that attitude determination will be done based on information from the magnetometer and sun sensors. A Kalman filter shall estimate directly the attitude quaternion obtained from attitude determination. The Kalman filter shall estimate as well the biases of the gyroscopes. The corrected gyro measurements will be employed in the Earth shadow where there are no solar sensor readouts and so the attitude cannot be determined. The attitude control consists of a negative feedback controller with output proportional to the pointing and the angular rate errors (Proportional-Derivative Control).

The next sections will present the kinematics and dynamics equations, the Kalman filter formulation for attitude estimation, the reduced order covariance matrix required to eliminate the singularity due to the quaternion, the mathematical models of the sensors and their errors, and the controller. The results are shown in sequel for both nominal and safe/acquisition modes.

2. Motion equations

The attitude of a satellite is defined as the orientation of a coordinate frame fixed on the satellite body with respect to an inertial reference frame. The relationship between the coordinate systems is done by means of rotation matrices, or co-sine direction matrix, which relate a vector in the inertial frame to the observed vector in the satellite frame. Only 3 parameters are needed in order

to univocally express the body attitude. Since the transformation matrix has 9 elements, 6 of them are mutually dependent from the others. It is practical, in this sense, to express the attitude by means of a reduced set of parameters like Euler angles, Euler axis and angle or quaternion, among several others [1], [2]. Quaternion is suitable for implementation on computing environments because it does not present singularities such as gimbal-lock or trigonometric functions, which require extra computational effort. As a drawback, quaternion has no direct physical interpretation of attitude, generally resolved by integrating the motion equations in quaternion and then converting it to Euler angles, which are physically more understandable. The quaternion has four elements, composed by a 3 dimensional vector and a scalar value:

$$\mathbf{q} = \begin{pmatrix} \boldsymbol{\varepsilon} & \eta \end{pmatrix}^T, \tag{1}$$

where $\boldsymbol{\varepsilon}$ is the vector and η is the scalar part of the quaternion. The quaternion has unit module, and therefore obeys the relationship $\boldsymbol{\varepsilon}^T\boldsymbol{\varepsilon} + \eta^2 = \varepsilon_1^2 + \varepsilon_2^2 + \varepsilon_3^2 + \eta^2 = 1$. The rotation matrix that relates the inertial frame to the body fixed frame can be expressed as a function of the quaternion [1], [3]:

$$\mathbf{C}_{bi} = (\eta^2 - \boldsymbol{\varepsilon}^T\boldsymbol{\varepsilon})\,\mathbf{1} + 2\,\boldsymbol{\varepsilon}\,\boldsymbol{\varepsilon}^T - 2\,\eta\,\boldsymbol{\varepsilon}^{\times}, \tag{3}$$

where $\mathbf{1}$ is the identity matrix of third order, and the superscript $\times$ denotes the anti-symmetric matrix of the cross product of vector $\boldsymbol{\varepsilon}$. The attitude matrix is such that a vector $\mathbf{r}_i$ expressed in the inertial frame is represented in the body fixed system by $\mathbf{r}_b = \mathbf{C}_{bi}\ \mathbf{r}_i$. The rotation matrix of attitude results:

$$\mathbf{C}_{ba} = \begin{pmatrix} \eta^2 + \varepsilon_1^2 - \varepsilon_2^2 - \varepsilon_3^2 & 2(\varepsilon_1\varepsilon_2 + \eta\varepsilon_3) & 2(\varepsilon_1\varepsilon_3 - \eta\varepsilon_2) \\ 2(\varepsilon_1\varepsilon_2 - \eta\varepsilon_3) & \eta^2 - \varepsilon_1^2 + \varepsilon_2^2 - \varepsilon_3^2 & 2(\varepsilon_2\varepsilon_3 + \eta\varepsilon_1) \\ 2(\varepsilon_1\varepsilon_3 + \eta\varepsilon_2) & 2(\varepsilon_2\varepsilon_3 - \eta\varepsilon_1) & \eta^2 - \varepsilon_1^2 - \varepsilon_2^2 + \varepsilon_3^2 \end{pmatrix}, \tag{4}$$

The kinematics equation of attitude when expressed in quaternion results in:

$$\dot{\mathbf{q}} = \frac{1}{2}\boldsymbol{\Omega}\,\mathbf{q}, \text{ where } \boldsymbol{\Omega} = \begin{pmatrix} -\boldsymbol{\omega}^{\times} & \boldsymbol{\omega} \\ -\boldsymbol{\omega}^T & 0 \end{pmatrix}, \tag{5}$$

with $\boldsymbol{\omega}$ being the angular velocity of the body in body-fixed coordinates relative to the inertial system. It is assumed in this work that the angular velocity comes from measurements of a set of 3 on-board gyroscopes aligned with body axes. It is also considered that the mathematical model of the gyroscope measurement is given by:

$$\tilde{\boldsymbol{\omega}} = \boldsymbol{\omega} + \mathbf{b} + \boldsymbol{\upsilon}, \tag{6}$$

where $\tilde{\boldsymbol{\omega}}$ gives the measured angular velocity vector, $\mathbf{b}$ is the gyroscope bias vector and $\boldsymbol{\upsilon}$ is a white noise representing the measurement uncertainties. Attitude determination shall be made with the coarse solar sensor readings and magnetometers, which will be processed by either TRIAD or QUEST algorithm [4], [5], [6] and [7].

The attitude dynamics is given by the Euler's differential equation for a rigid body, with the inclusion of the reaction wheel effects. The resulting differential model is expressed in body frame coordinates by

$$\begin{aligned} \mathbf{J}\,\dot{\boldsymbol{\omega}} &= \mathbf{g} - \boldsymbol{\omega} \times \left(\mathbf{J}\,\boldsymbol{\omega} + \mathbf{h}\right) + \mathbf{g}_w \\ \dot{\mathbf{h}} &= \mathbf{g}_w \end{aligned}, \tag{7}$$

where $\mathbf{g}$ is the sum of the external torques applied to the satellite, $\mathbf{J}$ is the satellite inertia, excluding the flywheel inertias around their axes [1], $\mathbf{h}$ is the total reaction wheel's angular momentum, and $\mathbf{g}_w$ is the torque applied to the reaction wheels by the attitude controller.

3. Kalman Filter Implementation for Attitude Determination

The Kalman Filter (KF) is an optimal recursive method for linear state estimation in presence of noisy measurements. The original formulation applies to linear dynamic systems, Refs. [8-9]. For spacecraft attitude estimation, where attitude sensors and gyros are available, it is customary to define the state vector composed by $\mathbf{x} \equiv (\mathbf{q}, \mathbf{b})$, i.e. quaternion and gyro biases (drifts), and work with reduced covariance to avoid the singular quaternion covariance. Here the formulation follows closely the scheme proposed in [8]. It is assumed that the stochastic ODEs of state are:

$$\dot{\mathbf{x}} = \begin{bmatrix} \dot{\mathbf{q}} \\ \dot{\mathbf{b}} \end{bmatrix} = \begin{bmatrix} \frac{1}{2}\boldsymbol{\Omega}\,\mathbf{q} \\ 0 \end{bmatrix} + \mathbf{w} \tag{8}$$

where $\mathbf{w}$ is the dynamical white noise representing uncertainties in the model, with covariance $\mathbf{Q}$, i.e. $\mathbf{w} = \mathrm{N}(0, \mathbf{Q})$. The discrete measurement model is given by:

$$\mathbf{y}_k = \mathbf{H}_k\ \mathbf{x}_k + \mathbf{v}_k\,, \tag{9}$$

where $\mathbf{H}_k = [\mathbf{I}_4\ \ \mathbf{0}_{4\times3}]$ is the measurement matrix, $\mathbf{y}_k$ is the output measurement vector, and $\mathbf{v}_k$ is the gaussian white noise with covariance matrix $\mathbf{R}_k$, i.e. $\mathbf{v}_k = N(0, \mathbf{R}_k)$. From here on, the standard Kalman filter could be used, however the quaternion covariance is singular which compromises the filter modeling. This problem will be dealt with in the formulation explained in the next section.

3.1. State Vector of the Filter

From the previous sections, a state vector for the attitude estimation can be chosen, based on the quaternion $\mathbf{q}$ and the gyro bias vector $\mathbf{b}$. Equation 5 gives the motion equations for these vectors and, by assuming that the satellite angular velocity is constant during two consecutive measures, it results $\dot{\mathbf{b}} = \mathbf{0}$. Therefore, the state is of 7^{th} order. Since it was assumed that $\boldsymbol{\omega}$ is constant between measurements, the quaternion kinematic equation and the biases can be predicted, resulting the discrete equation:

$$\bar{\mathbf{x}}_{k+1} = \begin{bmatrix} \bar{\mathbf{q}}_{k+1} \\ \bar{\mathbf{b}}_{k+1} \end{bmatrix} = \begin{bmatrix} \boldsymbol{\Phi}_q(\hat{\boldsymbol{\omega}}_k) & \mathbf{0} \\ \mathbf{0} & \mathbf{I}_{3\times 3} \end{bmatrix} \begin{bmatrix} \hat{\mathbf{q}}_k \\ \hat{\mathbf{b}}_k \end{bmatrix}, \tag{10}$$

where the quaternion transition matrix $\boldsymbol{\Phi}_q(\boldsymbol{\omega})$ can be obtained from [8]:

$$\boldsymbol{\Phi}_q(\boldsymbol{\omega}) = \cos\left(\frac{|\boldsymbol{\omega}|\,\Delta t}{2}\right)\mathbf{I}_{4x4} + \frac{1}{|\boldsymbol{\omega}|}\sin\left(\frac{|\boldsymbol{\omega}|\,\Delta t}{2}\right)\boldsymbol{\Omega}, \tag{11}$$

and where $|\boldsymbol{\omega}|$ is the magnitude of the angular velocity vector. This formulation, in terms of the transition matrix, is preferable than the traditional state differential equation since it avoids the numerical integration of the state. The state of the filter can process the measurements via:

$$\begin{aligned} \mathbf{K}_k &= \mathbf{S}(\bar{\mathbf{q}}_k)\,\tilde{\mathbf{K}}_k \\ \hat{\mathbf{x}}_k &= \bar{\mathbf{x}}_k + \mathbf{K}_k\left(\tilde{\mathbf{q}}_k - \bar{\mathbf{q}}_k\right) \end{aligned}, \tag{12}$$

where it is assumed that the measurement vector is the observed quaternion $\tilde{\mathbf{q}}_k$, and the gain $\tilde{\mathbf{K}}_k$ and matrix $\mathbf{S}(\mathbf{q})$ will be defined next. Wherever needed the corrected angular velocity from gyros may be rebuilt recalling Eq. 6, and using the estimated biases $\hat{\mathbf{b}}$:

$$\boldsymbol{\omega} = \tilde{\boldsymbol{\omega}} - \hat{\mathbf{b}}, \tag{13}$$

3.2. Reduced Order Filter Covariance

Since a complete attitude can be specified with only 3 scalar values, the quaternion representation is somewhat redundant. In fact, the four elements of a quaternion shall satisfy the condition of unit modulus, and therefore only 3 of them are really independent. This property produces a singular covariance matrix when the state vector contains the attitude quaternion. The covariance matrix in this case cannot be inverted and therefore the Kalman filter is useless. In practice, some small errors in the processing data allow to compute the inverse of the covariance matrix although with filter degradation. A different approach was suggested by [8] that consists of reducing the order of the covariance matrix. The covariance order is reduced from 7 to 6 degree, and now it has full rank. The reduced order covariance matrix has the form:

$$\mathbf{P}^r = \mathbf{S}^T(\mathbf{q})\,\mathbf{P}\,\mathbf{S}(\mathbf{q}), \tag{14}$$

where the superscript *r* means the reduced form, and **S** is a rectangular transformation matrix of order 7 × 6. Since the covariance shall be propagated, the dynamical noise covariance **Q** shall also have a reduced order, as

$$\mathbf{Q}^r = \mathbf{S}^T(\mathbf{q})\,\mathbf{Q}\,\mathbf{S}(\mathbf{q}). \tag{15}$$

The **S** matrix is built by

$$\mathbf{S}(\mathbf{q}) \equiv \begin{bmatrix} \boldsymbol{\Xi}(\mathbf{q}) & \mathbf{0}_{4x3} \\ \mathbf{0}_{3x3} & \mathbf{I}_{3x3} \end{bmatrix}_{7x6} \text{ with } \boldsymbol{\Xi}(\mathbf{q}) \equiv \begin{bmatrix} \eta & -\varepsilon_3 & \varepsilon_2 \\ \varepsilon_3 & \eta & -\varepsilon_1 \\ -\varepsilon_2 & \varepsilon_1 & \eta \\ \varepsilon_1 & -\varepsilon_2 & -\varepsilon_3 \end{bmatrix}_{4x3} \tag{16}$$

Now the Riccati equation can be used to propagate the reduced order covariance matrix, by means of [9]:

$$\overline{\mathbf{P}}_{k+1}^{r} = \tilde{\boldsymbol{\Phi}}\ \hat{\mathbf{P}}_{k}^{r}\ \tilde{\boldsymbol{\Phi}}^{T} + \int_{t_k}^{t_{k+1}} \tilde{\boldsymbol{\Phi}}\ \mathbf{Q}^{r}\ \tilde{\boldsymbol{\Phi}}^{T}\ dt\,. \tag{17}$$

where the reduced order transition matrix is defined by:

$$\tilde{\boldsymbol{\Phi}} = \begin{bmatrix} \boldsymbol{\Lambda} & \mathbf{K}^{*} \\ \mathbf{0}_{3x3} & \mathbf{I}_{3x3} \end{bmatrix}_{6x6}, \tag{18}$$

with the following definitions:

$$\boldsymbol{\Lambda} = \boldsymbol{\Xi}^{T}(\overline{\mathbf{q}}_{k+1})\ \boldsymbol{\Phi}_{q}(\hat{\boldsymbol{\omega}}_{k})\ \boldsymbol{\Xi}(\hat{\mathbf{q}}_{k}), \text{ and } \mathbf{K}^{*} = -\frac{1}{2}\int_{t_k}^{t_{k+1}} \boldsymbol{\Lambda}\ dt\,. \tag{19}$$

The measurement update phase of the reduced covariance may be computed through:

$$\begin{aligned} \tilde{\mathbf{H}}_{k} &= \mathbf{H}_{k}\ \mathbf{S}(\overline{\mathbf{q}}_{k}) \\ \tilde{\mathbf{K}}_{k} &= \overline{\mathbf{P}}_{k}^{r}\ \tilde{\mathbf{H}}_{k}^{T}\left(\tilde{\mathbf{H}}_{k}\ \overline{\mathbf{P}}_{k}^{r}\ \tilde{\mathbf{H}}_{k}^{T} + \mathbf{R}_{k}\right)^{-1}. \\ \hat{\mathbf{P}}_{k}^{r} &= \left(\mathbf{I}_{6x6} - \tilde{\mathbf{K}}_{k}\ \tilde{\mathbf{H}}_{k}\right)\overline{\mathbf{P}}_{k}^{r} \end{aligned} \tag{20}$$

Within this procedure, once the reduced covariance is set at the beginning, the full covariance does not need to be reconstituted.

3.3. Sensor models, quaternion measurements, and filter setup

Attitude determination of CONASAT will rely on a tri-axis magnetometer and a set of 6 coarse analog solar sensors, in each satellite face. Solar sensor readings are proportional to the co-sine of the incident angle, and converted to a unit vector of the sun direction after being processed by the on-board attitude determination software. It is assumed in simulation that this unit vector was already computed so the simulated sensor model is given by

$$s_i = u_i(1+\tau_i) \tag{21}$$

where s_i, i = 1, 2, 3, is the simulated measured sun direction in body frame coordinates, $\mathbf{u} = (u_1, u_2, u_3)$ is the sun direction and τ_i is a zero mean white noise with 0.5°/h standard deviation. It can be noted that the measured model of the sun sensor is not a simple additive noise. The reason for that is that there are no negative readings in the solar detector, and the noise decreases with sun intensity on the cell. The measured sun direction unit vector is computed by

$$\mathbf{s}_s = \frac{1}{\sqrt{s_1^2 + s_2^2 + s_3^2}} \begin{pmatrix} s_1 & s_2 & s_3 \end{pmatrix}^T \tag{22}$$

Although the sun sensor model is different from the linear model usually employed in Kalman filter, it is expected that the filter still converge to the true solution, since this model still preserves the real sensor behavior. On the other hand, the magnetometer mathematical model is composed by a noise and small residual bias, because the magnetometer bias is normally estimated on ground, prior to launch:

$$\mathbf{m} = \mathbf{B} + \mathbf{b}_m + \boldsymbol{\upsilon}_m \tag{23}$$

where $\mathbf{B}$ is the Earth's magnetic field in body fixed coordinates, and $\mathbf{b}_m$ and $\boldsymbol{\upsilon}_m$ are the bias and white noise, respectively. The bias considered in simulation was $\mathbf{b}_m = (400\ -300\ 200)^T$ nT, while the noise standard deviation was σ_m = 100 nT. A similar model was also considered in the gyroscope unit, in which the angular velocity readings is composed by the true angular rate added to a bias and a white noise, in the form

$$\boldsymbol{\omega} = \mathbf{w} + \mathbf{b}_g + \boldsymbol{\upsilon}_g\,, \tag{24}$$

where $\mathbf{w}$ is the simulated angular rate, $\mathbf{b}_g = (50\ \ 50\ \ 50)^T$ °/h is the gyro bias to be estimated by the Kalman filter and $\boldsymbol{\upsilon}_g$ is a zero mean white noise with adopted standard deviation σ_g = **5**°/h.

The sensor measurements (magnetometer and sun sensors) where pre-processed to generate the quaternion measurement $\tilde{\mathbf{q}}$, to be used in the Kalman filter. A TRIAD algorithm was used to obtain the attitude matrix and then the quaternion, although QUEST could be used as well with equivalent results [4], [5] and [6]. The corresponding covariance $\mathbf{R}_k$ in a first approach should be a full matrix [4]; however to speed up the Kalman filter algorithm it was tuned to a constant 4th order diagonal matrix with elements equal to 0.0001.

The initial covariance matrix $\mathbf{P}_o$ was assumed to be a diagonal 7th order matrix with quaternion variance elements equal to 0.0025 and the gyroscope bias variance elements equal to 0.001 $(\text{rad/s})^2$. The dynamic noise covariance matrix $\mathbf{Q}$ was tuned constant as well and diagonal with elements equal to 10^{-4} for the quaternion terms and 10^{-10} for the gyro bias terms.

4. Attitude Control

Due the symmetric mass properties of CONASAT, it is suggested that the attitude control be based on a PID controller, with equal gains for all three axis. Although the PID controller theory applies just to linear systems, and considering that the satellite attitude dynamics is non-linear, it is well known that the PID still is able to stabilize and to control the attitude, even if large attitude errors are present. In order to make the onboard control software as simple and reliable as possible, the attitude error is computed as the Euler angles that come from a 1-2-3 (or yaw-roll-pitch) rotation [1] with respect to the local orbital frame. The applied control torque at time t_k is then given by:

$$\mathbf{u}_k = -k_p\ \boldsymbol{\theta}_k - k_i \sum_{i=0}^{k} \boldsymbol{\theta}_i\ \Delta t - k_d\ \boldsymbol{\omega}_k\ , \tag{25}$$

where k_p, k_i and k_d are the proportional, integral and derivative gains, respectively, and Δt is the control step time. The angular velocity $\boldsymbol{\omega}_k$ at time t_k is computed by the measured satellite angular velocity $\boldsymbol{\omega}$ corrected for the estimated bias $\mathbf{b}_g$. The integral error is calculated as a simple sum of the previously estimated Euler angles. It shall be noted that the attitude is computed with the estimated quaternion and the position of the satellite in its orbit, since CONASAT shall be Earth pointed. It is assumed that the orbit is propagated onboard by a Brower's analytical model [10]. The satellite position error was not considered in simulation, i. e, the simulated onboard orbit was considered perfect. The PID gains were manually adjusted to get an overdamped response to a step input, and resulted k_p = 0.006 Nm/rd, k_d = 0.08 Nms/rd and $k_i = 4 \times 10^{-5}$ Nm/rd s. The control torque was then applied to the reaction wheels, with axis aligned to the satellite frame. It was assumed that the applied torque is equal to the reaction wheel net torque, so the wheel's non-linearities and frictions were neglected. The maximum torque that the reaction wheel's can provide was considered equal to 625 μNm, and the wheel's maximum storage momentum is 0.0118 Nms.

The filter updates the attitude during the sunlight part of the orbit, where the attitude can be determined. In the shadowed part of the orbit, the attitude is computed by the corrected and integrated gyroscope measurements.

A residual magnetic torque was the only source of attitude disturbance in simulation. It was assumed that the satellite has a residual magnetic moment of $\mathbf{m}_r = (0.01\ -0.01\ 0.005)^T$ Am, a very large moment, indeed, that favors simulation confidence. Disturbance torque was computed by the cross product between the magnetic moment and the Earth's magnetic field strength **B** in body frame coordinates.

5. Nominal operating mode

Choosing the orbit elements of a small satellite is always a big problem, like in CubeSats. In fact, most CubeSats are launched as pig back in large launchers, and therefore the nanosats have to accept the orbit of the principal payload. However, the specified orbit for CONASAT is close to the orbit of the satellites SCD1 and SCD2 (circular at 750 km altitude, 25° inclination), which maximizes the ground contact of the satellites with the remote platforms. There are no guarantees, nevertheless, that this orbit will be fulfilled, since it will depend on launcher availability. The adopted orbit in simulation was circular, 630 km altitude and 25° inclination.

The initial attitude was set as $(60° \ 30° \ 40°)^T$ Euler angles of a 1-2-3 rotation sequence, with angular speed of $\boldsymbol{\omega} = (0.6 \ 0.3 \ 0.9)^T$ rpm. It was assumed that the attitude control during attitude acquisition could deliver the satellite from a random rate up to 5 rpm in any direction to less than 1 rpm in any axis. The resulting angular momentum after attitude acquisition can be stored in the reaction wheels and therefore the operation mode can be switched to nominal mode. Since at the present moment there still lack of detail on satellite mass and inertia, it was assumed that CONASAT mass shall be around 8.2 kg, due to the fact that it is composed by 8 CubeSats, each one with 1 kg mass, according to CubeSat specification. This mass was assumed as distributed on a cube of 0.2 m size, with small asymmetry, resulting a diagonal inertia tensor with principal inertia moments of 0.0547, 0.0519 and 0.0574 kg m^2, around the x, y and z satellite axis, respectively. The simulation process was carried out for 18000 seconds, or 3 orbits, approximately. The CONASAT shall be Earth pointed, which means that the reference for attitude control is the local orbital frame, with x axes pointing towards the zenith direction, z is parallel to the orbit angular momentum, and y completes the right handed system, and points towards the satellite velocity with respect to Earth in a circular orbit. During this period the satellite pass 3 times through the Earth shadow, at simulation times of 2240, 8065 and 13890 seconds, and with duration of 2130 seconds each, approximately. In the Earth eclipse, it is assumed that no attitude determination is performed, so no filter update of the quaternion and gyro biases will be done, although the attitude filtering continues to propagate the attitude. It is expected, therefore, that the attitude error start to increase as the satellite enter in the Earth shadow.

Figure 2 presents the estimated satellite attitude with respect to the local orbital frame for the first 300 seconds of simulation. The attitude is given as the Euler angles of a 1-2-3 rotation (yaw-roll-pitch). It can be seen that the reaction wheels absorb the satellite momentum and they manage to control and to point the satellite to the right position. It is still to be analyzed the robustness of the control, since the control gains were adjusted to give the best response for the initial conditions adopted in this particular simulation.

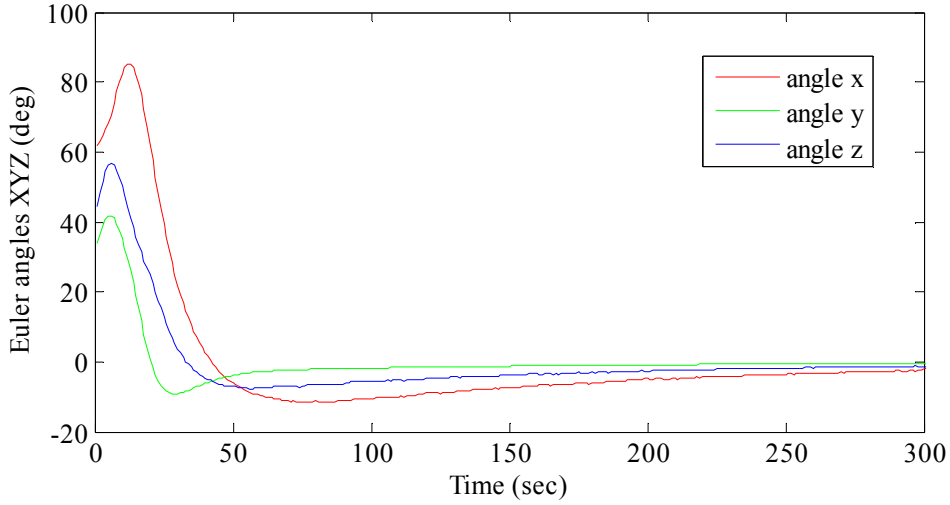

Figure 2. Estimated attitude during control starting up.

The computed attitude error of the estimation process is shown in Fig. 3. It is noticeable that the error remains small when compared with the attitude pointing requirements of 5° off the Nadir direction for *x* axes. The error is shown in Euler angles rather than quaternion, in order to make visualization easy. Although the error drifts in the Earth shadow, it becomes less than 2° after the second eclipse where the satellite is already rotating around its *z*-axis in synchronicity with the orbital motion and, therefore, assuring gyroscope stabilization in this axis.

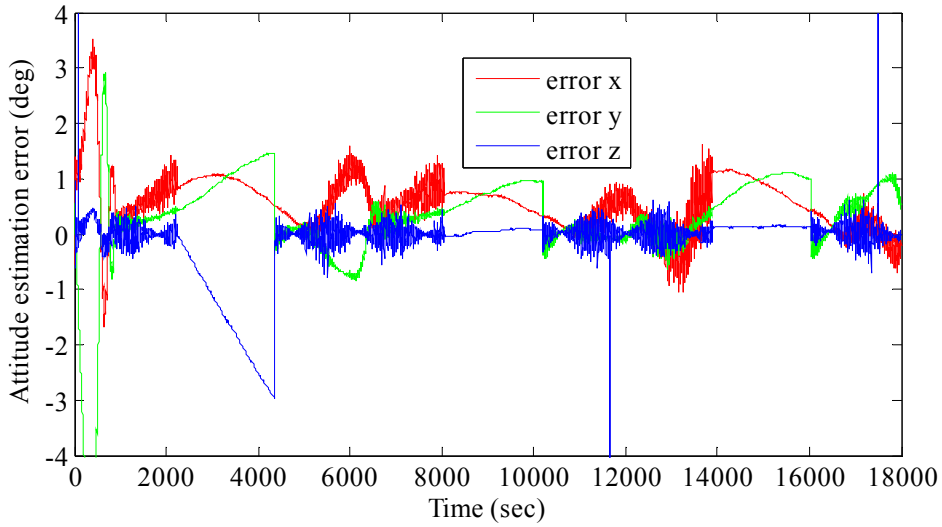

Figure 3. Estimated attitude error in Euler angles of a 1-2-3 transform.

The estimated gyroscope biases are shown in Fig. 4. After initialization with null values, the convergence reaches 90% of the final value after 37 minutes, just before entering the first Earth eclipse. A snap shot of the simulated gyro measurements for the interval 0 to 5000 seconds is shown in Fig. 5. The 0.01 rpm angular velocity of the orbital motion can be easily identified in the *z*-gyro measurements, while the remaining axes measurements are close to zero.

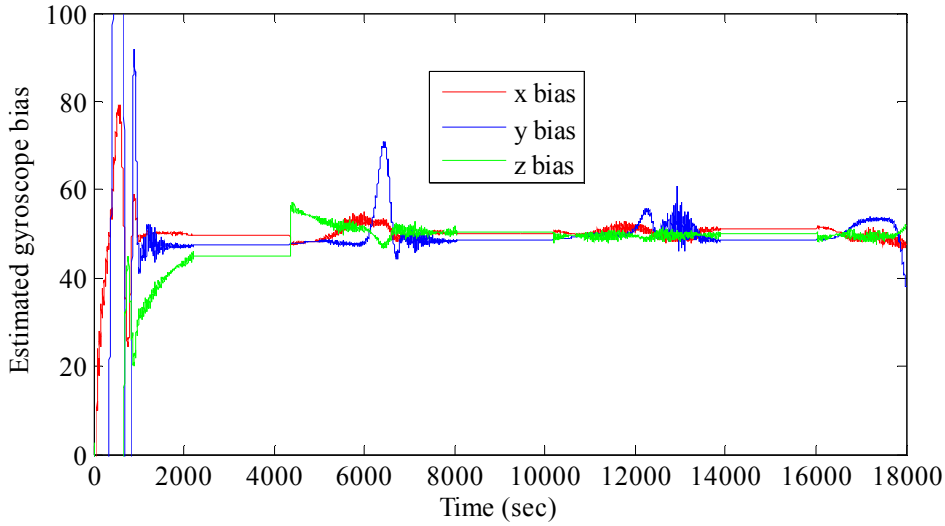

Figure 4. Estimated gyroscope biases

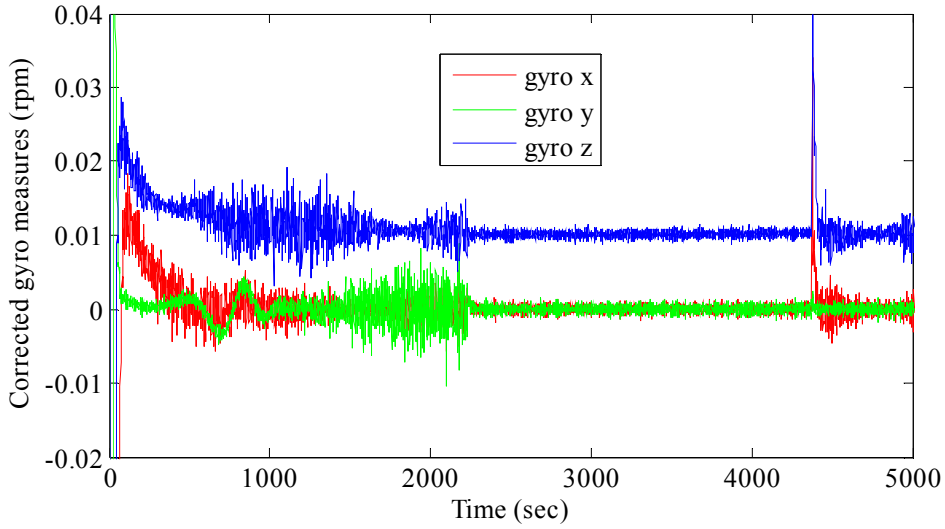

Figure 5. Corrected gyroscope measurements.

Figure 6 depicts the reaction wheels angular velocities under action of the attitude control. It can be noted that the residual magnetic torque causes the wheels to speed up, particularly in the *z* axes. The onboard torque coils will perform wheel de-saturation, but in this simulation the de-saturation was not included. The reaction wheel torque is presented in Fig. 7, for the first 300 seconds of simulation. Just after the attitude control starts to act on the satellite, the required torque is high and, therefore, the maximum reaction wheel allowed torque of 0.625 mNm is reached. After 20 seconds the wheels manage to absorb the satellite momentum and the torque starts decreasing to almost null. The small but significant steady state random torque of the reaction wheels showed in simulation can be explained by the remaining attitude and angular rate measurement noises. It is expected that this noise can be filtered through measurement filtering and by increasing the measurement rate.

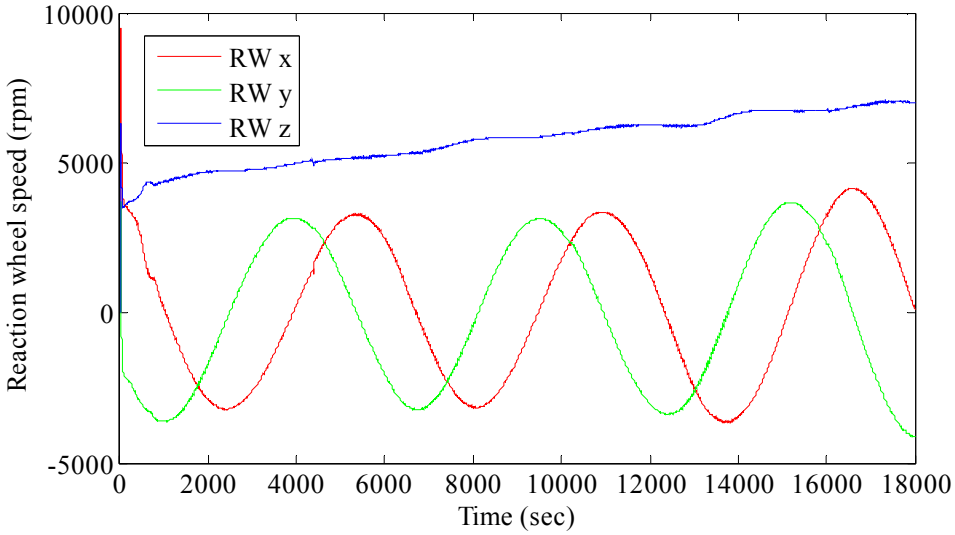

Figure 6. Reaction wheel angular speed.

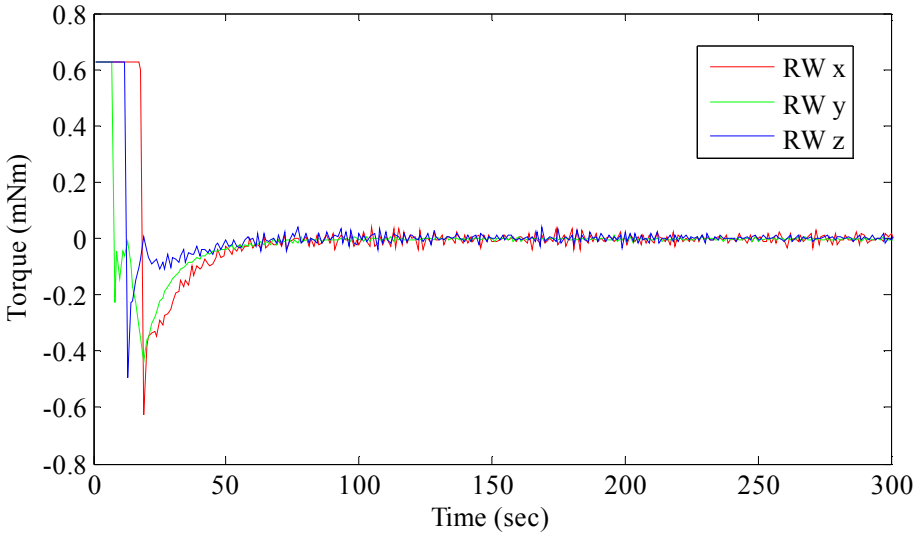

Figure 7. Reaction wheel torque.

6. Attitude acquisition and safe modes

For the attitude acquisition and safe modes there are no fully established requirements yet. It is believed that these methods have at least to provide sun pointing to deliver the required energy for safe operation of the satellite, and to stabilize the attitude in order to permit transferring the satellite to nominal operating mode. In both attitude acquisition and safe modes, it is appropriate that the satellite points the communication antenna to Earth to enable a high gain link, and it is necessary that the angular rate be kept below an acceptable maximum value. Therefore, the following conditions for the acquisition and safe modes were established: the attitude control satellite should reduce any angular rate with respect to the local orbital reference system, and the controller should point the face containing the antennas to Earth, which implies in roll and pitch control. Although there is no imposition for yaw control, it was included in the simulations shown here. The attitude control system will rely on solar sensors and magnetometer to perform the attitude determination, and magnetic torque coils to provide control action; the reaction wheels will not be used in these operating modes. The gyros also shall not be used, since they have high drift and the gyro biases will not be estimated in these modes. It shall be pointed out that these operation modes differs from that usually employed in CubeSats, which is based exclusively on the magnetometer without any attitude determination algorithm, and can just dampen the angular velocities relative to the Earth's magnetic field. In the operating mode suggested here a complete attitude determination and control is performed during the illuminated part of the orbit, while during the eclipse a Bdot algorithm executes a rate reduction. The attitude determination was simulated with the TRIAD method, without any filtering. The angular velocity necessary to the controller will be calculated by a numerical derivation of the attitude matrix as explained in the following. The magnetometer and the solar sensor measurements provide two non-collinear vectors in the satellite reference system for the TRIAD method. The vectors are then normalized and allow the construction of an intermediate coordinate system BS for each pair of vectors. The BS base vectors constitute the transformation matrix $\mathbf{C}_{BSb}$ between the satellite reference system and BS, and so the satellite attitude is now known in the BS system. The sun direction and the geomagnetic field vectors will also be calculated by the onboard computer provided the satellite position in its orbit is known, based on analytical models

of the Earth's magnetic field and the position of the Sun relative to Earth. Again, these pair of vectors makes possible to compute a new attitude matrix, $\mathbf{C}_{BSi}$, which relates the inertial system to BS reference system. The onboard orbit propagation also allows calculating the $\mathbf{C}_{io}$ matrix between the inertial frame and the local orbital system. The attitude matrix between the satellite and the local orbital systems, $\mathbf{C}_{bo}$, can now be calculated by:

$$\mathbf{C}_{bo} = \mathbf{C}_{BSb}^{T}\,\mathbf{C}_{BSi}\,\mathbf{C}_{io}\,, \tag{26}$$

The angular velocity of the satellite is given by [1], [2]

$$\boldsymbol{\omega}^{\times} = -\dot{\mathbf{C}}_{bo}\,\mathbf{C}_{bo}^{T}\,. \tag{27}$$

where the superscript × denotes the vector product matrix built from the vector $\boldsymbol{\omega}$. It is admitted here that the derivative of the attitude matrix can be approximated by the difference between two matrices calculated at different times:

$$\dot{\mathbf{C}}_{bo} \cong \frac{\mathbf{C}_{bo}(t) - \mathbf{C}_{bo}(t-\Delta t)}{\Delta t}, \tag{28}$$

but if Δt is small the derivative will be affected by the noise presence in the measurements, and the error in the computed angular velocity will be large. On the other hand if Δt is large, or, equivalently, if the angular speed is high, the error tends also to increase because $\boldsymbol{\omega}$ is not constant in body fixed frame. There is, therefore, a compromise between the maximum allowed numeric derivative error and the time interval Δt. It is suggested here that time interval be calculated based on the previous value of the angular velocity of the form:

$$\Delta t_k > \frac{\Delta\theta}{\left|\boldsymbol{\omega}_{k-1}\right|}, \tag{29}$$

where the subscript k refers to instant at which the time interval Δt is calculated. This simple procedure proved to be important in reducing the time spent on attitude acquisition. The increment angle $\Delta\theta$ was adjusted in the simulation and reached out a good performance when $\Delta\theta \approx 0.6^{o}$. Between two successive calculations of Δt the previously computed angular velocity vector $\boldsymbol{\omega}$ by Eq. 27 is kept constant, although the attitude is updated at every sensor reading. Control output is then achieved by Eq. 25 with Euler angles obtained from the $\mathbf{C}_{bo}$ attitude matrix [1]. However, for attitude acquisition and safe modes a Proportional-Derivative controller will be employed instead of a PID, whose gains are, respectively, k_p = 0.0008 Nm/rd and k_d = 5 Nms/rd. Since the torque generated by the magnetic coils is perpendicular to the Earth's magnetic field, then the commanded magnetic moment to the coils must be calculated through:

$$\mathbf{m} = \frac{\mathbf{B}\times\mathbf{u}}{\left|\mathbf{B}\right|}, \tag{30}$$

where $\mathbf{m} = (m_1 \quad m_2 \quad m_3)^T$ is the magnetic moment be commanded to the torque coils, with restriction that $-m_{max} < m_i < m_{max}$, (i = 1, 2, 3) with m_{max} = 0.07 Am^2, and $\mathbf{B}$ is the Earth's magnetic field in satellite coordinates. To prevent the control continuing to operate when the attitude is already stabilized, a dead zone of 5^o in attitude was introduced in the controller within which the control is turned off.

During eclipse periods, in which the satellite is in Earth's shadow, the attitude controller relies on the Bdot method [11], [12] to perform attitude detumbling by reducing the satellite angular rate, calculated by means of:

$$\dot{\mathbf{B}} \cong \frac{\mathbf{B}(t) - \mathbf{B}(t - \Delta t)}{\Delta t}, \tag{31}$$

where and so attitude pointing is not accomplished in the Earth shadow. A simple derivative controller with k_d gain of 5 Nms/rd is then used to deliver the required torque by

$$\mathbf{m} = -k_d \frac{\dot{\mathbf{B}}}{|\mathbf{B}|}, \tag{32}$$

The results of the simulated attitude acquisition are shown in Fig. 8 to 10. Figure 8 presents the detumbling phase for a initial rate of 5 rpm. In the simulation shown in Fig. 8 the conditions necessary for nominal mode switching are reached after 2 hours, but the time spent on detumbling depends on the attitude and angular rate just after launcher separation. The control torque is presented in Fig. 9, where the torque is calculated by

$$\mathbf{g}_{cont} = \mathbf{m} \times \mathbf{B}. \tag{33}$$

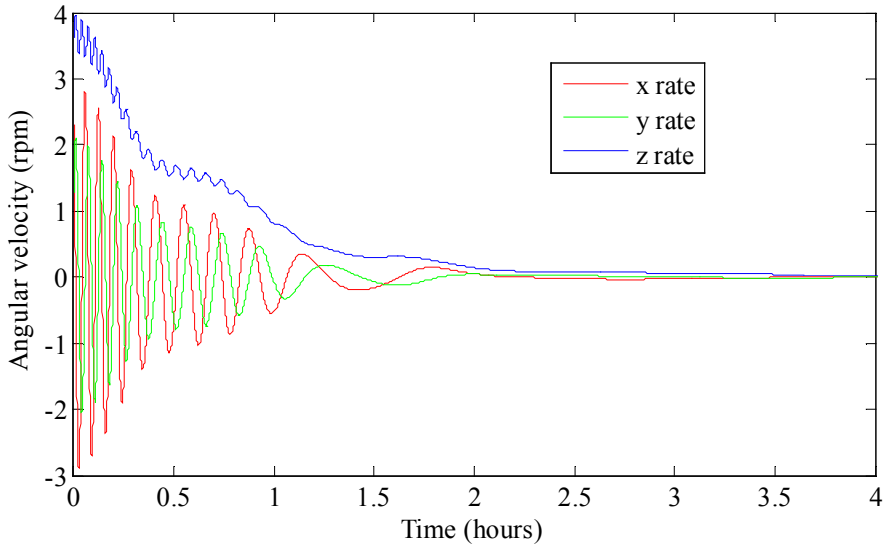

Figure 8. Satellite angular rate during attitude acquisition.

This torque was the only source of external torques used in the simulation of the attitude acquisition mode. The attitude error during attitude acquisition can be seen in Fig. 10. The error was calculated with the Euler angle θ from a Euler axis and angle representation of the attitude [1]. Although attitude stabilization is achieved after just 2 hours, it is necessary almost 8 hours to drive the satellite to the right attitude, in this particular simulation, as can be noted in Fig. 10. The time spent in the whole attitude acquisition phase is in accordance with the CONASAT requirements for power availability for early orbits.

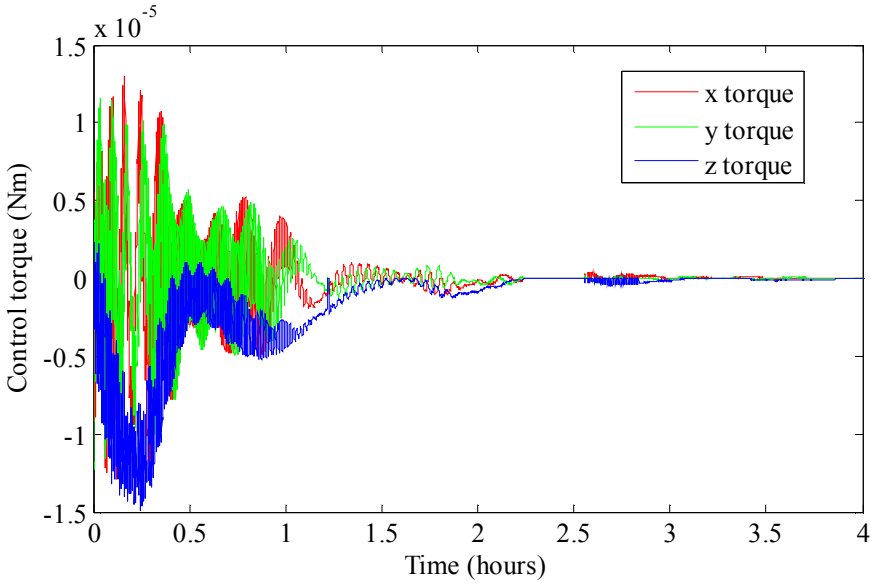

Figure 9. Control torque during the simulated attitude acquisition.

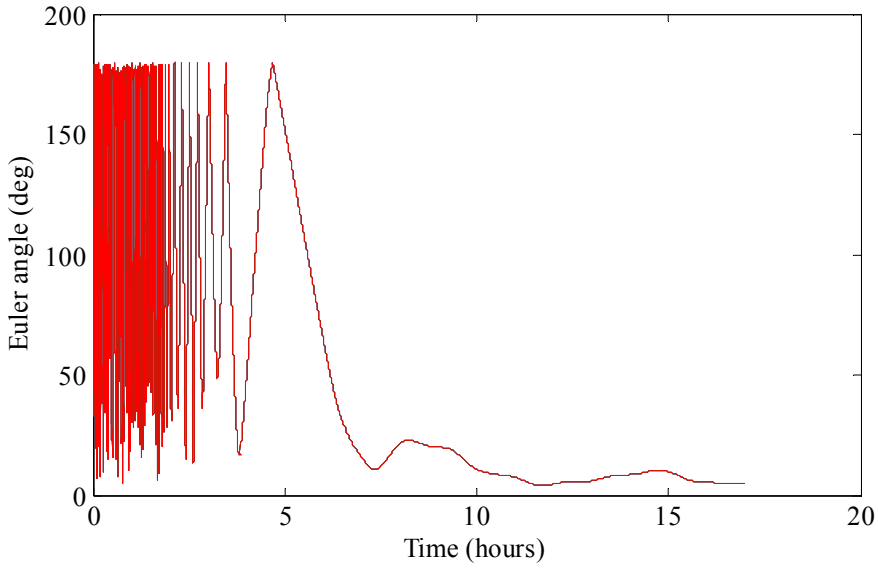

Figure 10. Attitude error during simulation of the attitude acquisition mode.

7. Conclusions

This paper presented simulations of the attitude controller for the satellite CONASAT satellite, a 8U class of the CubeSat system. The simulations were carried out for two operating modes: nominal mode and attitude acquisition mode along with safe mode. The control system proposed in this paper was able to provide the CONASAT with a very accurate and reliable controller, even considering that the available sensors of CONASAT for attitude determination and control are imprecise. The nominal operating mode controller showed a very fast time response, with a steady state error of less than 2°, and the controller reached the expected performance for this kind of satellite. Still remains to be studied the small jitter caused by the control action due to the noise present in the sensor measurements. A more realistic model of the reaction wheels shall be included in future simulations, since this work considers the wheels as ideal, which means that the wheels can deliver the required torque at the very precise time. It shall also be included in the next simulations the de-saturation process of the reaction wheels through the magnetic torque coils.

The simulation of attitude acquisition has shown that the detumbling phase can last at least 2 hours after orbit injection and satellite deployment from launcher. At the end of this phase, the satellite angular rate is small and the nominal operating mode can be switched on, with the reaction wheels absorbing the remaining momentum of the satellite. However, the final attitude specified for safe mode is reached only 8 hours after satellite injection considering an initial angular speed of 5 rpm.

The proposed attitude control system meets the current requirements of CONASAT and should be taken as a reference to the design phase and developments needed for the satellite.

8. References

[1] Hughes, P. C. “Spacecraft Attitude Dynamics”. Mineola: Dover, 1986.

[2] Wertz, J. R. “Spacecraft attitude determination and control”. D. Reidel Publishing, 1978.

[3] Carrara, V. “Cinemática e dinâmica de satélites artificiais”. São José dos Campos: INPE, 2012. 111 p. (sid.inpe.br/mtc-m19/2012/01.26.19.13-PUD). <http://urlib.net/8JMKD3MGP7W/3B96GD8>.

[4] Shuster, M. D. and Oh, S. D. “Three-Axis Attitude Determination from Vector Observations”. Journal of Guidance, and Control. Vol. 4, No. 1, 1981, pp. 70-77.

[5] Markley, F. L. and Mortari, D. “Quaternion attitude estimation using vector observations”. Journal of the Astronautical Sciences, Vol. 48, No. 2, 2000, pp. 359-380.

[6] Markley, F. L. “Attitude Determination Using Vector Observations: A Fast Optimal Matrix Algorithm”. Journal of the Astronautical Sciences, Vol. 41, No. 2, 1993, pp. 261-280.

[7] Yun, X., Bachmann, E. R. and McGhee, R. “A Simplified Quaternion-Based Algorithm for Orientation Estimation From Earth Gravity and Magnetic Field Measurements”. IEEE Transactions on Instrumentation and Measurement. Vol. 57, No. 3, 2008, pp. 638-650.

[8] Lefferts, E. J. Markley, F. L. Shuster, M. D. “Kalman filtering for spacecraft attitude estimation”, Journal of Guidance, Control, and Dynamics, Vol. 5, No. 5, 1982, pp. 417-429. DOI: 10.2514/3.56190.

[9] Garcia, R. V., Kuga, H. K. Zanardi, M. C. “Filtro não linear de Kalman Sigma-Ponto com algoritmo unscented aplicado a estimativa dinâmica da atitude de satélites artificiais”. Instituto Nacional de Pesquisas Espaciais. São José dos Campos/SP, 2011.

[10] Brower, D. “Solution of the Problem of Artificial Satellite Theory without Drag”. The Astronomical Journal, Vol. 64, No. 1274, Nov. 1959, pp. 378-397. DOI: 10.1086/107958.

[11] Reijneveld, J. and Choukroun, D. “Attitude Control System of the DELFI-N3XT Satellite”. Progress in Flight Dynamics, GNC, and Avionics, Vol. 6, 2013, pp. 189-208. DOI: 10.1051/eucass/201306189.

[12] Torczynski, D. M., Amini, R. and Massioni, P. “Magnetorquer Based Attitude Control for a Nanosatellite Testplatform”. AIAA Infotech Aerospace 2010, Atlanta, 2010. (AIAA 2010-3511).

9. Acknowledgements

The authors are grateful to the SIA and CONASAT projects, both funded by Finep (Brazil).